








Original Article

The Optimum Concentration of N-Methyl D-Aspartate to Induce Dorsal Root Ganglion Neuron Activation through the N-Methyl D-Aspartate Receptor Pathway: Creating a Neuron Model for the in-vitro Study of Pain

Ristiawan M Laksono^{1,2*} , Handono Kalim³ , Mohammad S Rohman⁴ , Nashi Widodo⁵ , Muhammad R Ahmad⁶ , Fa'urinda Riam Prabu Nery² , Willy Halim⁷ 

Abstract

Background: In the in-vitro study on chronic pain, the N-methyl D-Aspartate receptor (NMDAR) activation in the dorsal root ganglion (DRG) neuron became one of the most important mechanisms to activate the chronic pain pathways. NMDAR activation can be induced using an NMDAR agonist. No guidelines explain the NMDA optimum concentration to induce DRG neuron activation through the NMDAR pathway. This study aims to find the optimum concentration of NMDA to induce DRG neuron activation through the NMDAR pathway.

Materials and Methods: We treat DRG neuron culture derived from the F11 cell line with 10, 20, 40, 60, 80, and 100 μ M NMDA. Phosphorylated extracellular signal-regulated kinase (pERK), an activated neuron biomarker, is measured using an immunocytochemistry assay as a neuron activation biomarker. We validate the NMDA optimum concentration by measuring intracellular Ca^{2+} level, mitochondrial membrane potential ($\Delta\psi_m$), and cytosolic adenosine triphosphate (ATP) in the activated neuron. Those parameters are the downstream process following NMDAR activation and are related to neuron activity. Statistical analysis was performed using the One-Way ANOVA test with $\alpha=5\%$.

Results: We found that NMDA 80 μ M significantly had the highest pERK intensity and showed the most optimum neuron activation. Validation tests show an increase in intracellular Ca^{2+} influx and $\Delta\psi_m$. NMDA 80 μ M also causes significant depletion in the cytosolic ATP concentration related to neuron activation. NMDA 80 μ M induces neuron activation by increasing pERK, Ca^{2+} influx, $\Delta\psi_m$, and cytosolic ATP depletion.

Conclusion: NMDA 80 μ M is the optimum concentration to induce DRG neuron activation through the NMDA receptor pathway.

Keywords: DRG neuron, NMDA, pERK, calcium influx, ATP, mitochondrial membrane potential

1. Doctoral Program in Medical Science, Faculty of Medicine, Brawijaya University, Indonesia
2. Department of Anesthesiology and Intensive Therapy, Faculty of Medicine, Brawijaya University, Indonesia.
3. Department of Internal Medicine, Faculty of Medicine, Brawijaya University, Indonesia.
4. Department of Cardiology and Vascular Medicine, Faculty of Medicine, Brawijaya University, Indonesia.
5. Department of Biology, Faculty of Mathematics and Natural Science, Brawijaya University, Indonesia.
6. Department of Anesthesiology, Intensive Care and Pain Management, Faculty of Medicine, Hasanuddin University, Indonesia.
7. Departement of Medicine, Faculty of Medicine Brawijaya University, Indonesia.

Corresponding Author: Ristiawan Muji Laksono, Department of Anesthesiology and Intensive Therapy, Faculty of Medicine, Brawijaya University, Indonesia. phone: +6281233773593.
Email: ristiawanm@ub.ac.id

Please cite this article as: Laksono RM, Kalim H, Rohman MS, Widodo N, Ahmad MR, Nery FRP, et al. The Optimum Concentration of N-Methyl D-Aspartate to Induce Dorsal Root Ganglion Neuron Activation through the N-Methyl D-Aspartate Receptor Pathway: Creating a Neuron Model for the in-vitro Study of Pain. J Cell Mol Anesth. 2023;8(4):221-30. DOI: <https://doi.org/10.22037/jcma.v9i1.42426>

The "Journal of Cellular and Molecular Anesthesia" is licensed under a Creative Commons Attribution-NonCommercial 4.0 International License
 Vol 8, No 4, Fall 2023

Introduction

Chronic pain formation is related to N-Methyl D-Aspartate receptor activation (1). NMDAR is an ionotropic glutamate receptor that underlies many physiological processes in neurons (2). In the neuron, NMDAR is activated by the neurotransmitter glutamate following neuron depolarization due to the activation of co-receptor α -amino-3-hydroxy-5-methyl-4-isoxazole-propionate (AMPA) (3). NMDAR activation activates the downstream reaction, including activation of the Mitogen-activated protein kinases (MAPKs), one of the pain pathways. NMDAR activation promotes Ca^{2+} influx, which activates PKC, Src, Raf-1, MEK, and ERK. A phosphorylated extracellular signal-regulated kinase contributes to the expression of several genes related to long-term synaptic plasticities, such as NK-1, Cox-2, c-fos, Zif268, pro-Dyn, and TrkB, which induce and maintain neuron sensitization (4). pERK is also highly expressed in the dorsal root ganglion following the noxious stimulus (5). Phosphorylated ERK becomes a reliable biomarker of neuron activity and central sensitization (6). Neuron activation also affects other mechanisms, such as mitochondrial energy generation. Neuronal activation promotes metabolic activity such as ATP generation. (7) The increase of Ca^{2+} influx following NMDAR activation also increases ATP production through the tricarboxylic acid cycle (Kreb cycle) enzymatic activity (8, 9).

The dorsal root ganglion neuron, a primary neuron isolated from the dorsal root ganglion located in the peripheral nervous system, is one of the sensory neurons commonly used in in-vitro studies related to pain (10, 11). DRG neurons play a critical role in developing chronic/neuropathic pain and hyperexcitability (peripheral sensitivity) to tissue damage or inflammation in the onset and management of chronic pain (12). DRG neurons detect stimuli and send the signals to the central nervous system (13). This knowledge leads scientists to establish studies on the potential of DRGs as therapeutic targets of chronic pain therapy (12). Several mechanisms related to chronic pain occur in the DRG, including the progression of ectopic neuron activity, peripheral sensitization, gene regulation, presynaptic modulation,

phenotypic switch, and presynaptic modulation (12).

In the in-vitro study, NMDAR activation could be induced by administering NMDAR agonist glycine, glutamate, or NMDA (14). Compared to glutamate, NMDA is more potent to use as an NMDAR agonist since it has a lower affinity for the plasma membrane transporters. NMDA is also selective to NMDAR. NMDA binds to the glycine binding domain, GluN1, contributing to the NMDAR activation (15). NMDA also could bind to the NR2 subunit, a glutamate residue that responds to the channel opening (16). In the in-vitro study related to pain, DRG neuron activation becomes a necessary aspect and could be used in determining the pain or pain treatment mechanism. There are no specific guidelines for NMDA concentration in activating NMDAR. Therefore, this study aims to determine the optimum concentration of NMDA to induce dorsal root ganglion neuron activation through the NMDAR pathway.

Methods

This study was approved by the Brawijaya University Ethical Clearance Committee (No. 114-KEP-UB-2020).

Cell line F-11 differentiations become mature dorsal root ganglions: We used differentiated DRG neurons derived from cell line F-11 (08062601, Sigma). The F-11 cell culture method refers to Hashemian *et al.* with modifications (17). Cell line F11 was cultured in Ham F-12 medium, 10% Fetal bovine serum (FBS), HAT medium (sodium hypoxanthine five mM, aminopterin 20 μM , and thymidine 0.8 mM), 100 U/ml penicillin and 100 $\mu\text{g}/\text{ml}$ streptomycin. Cells were cultured in 25 cm^2 flasks in the cell culture incubator with 5% CO_2 at 37°C. Subculture was performed when the cells reached 60-70% of the bottom of the flask. Cell differentiation referred to the method of Pastori *et al.* (18). Cells were cultured at 2.5×10^5 cells/ml for 24 hours in six-well plates with Ham F-12 media. Then the media was changed to a differentiation medium consisting of Dulbecco's modified eagle medium (DMEM), 1% FBS, two mM glutamine, 100 U/ml penicillin, and 100 g/ml streptomycin. The media was changed every two days,

and cells were cultured for 12 days. DRG characterization approved morphological and biomolecular approach using neuronal marker microtubule-associated proteins 2 (MAP2). Morphology observation and MAP2 measurement were done on cell culture on days 0, 4, 5, 10, and 12.

Microtubule-associated proteins 2 (MAP2) examination: MAP2 measurement using primary antibody anti-MAP2 (GTX50810, GeneTex, USA). Neurons are differentiated in 24 well-plates. The treated cells were fixed. The aspirated cell medium was added 2-3 mm above the cell surface 4% formaldehyde in 1x Phosphate-buffered saline (PBS). Cells were fixed for 15 minutes at room temperature. The fixative was aspirated, and then the cells were washed three times using 1 X PBS for 5 minutes for each wash. The next stage was immunostaining. Cells were added with 100% cold methanol until submerged (3-5 mm), then incubated for 10 minutes at -20 °C and washed in 1x PBS for 5 minutes. Cells were supplemented with blocking buffer 1x PBS/ 5% normal serum / 0.3% Triton™ X-100). The blocking buffer was aspirated, and then the primary antibody was added with a 1:200 dilution in antibody dilution buffer (1X PBS / 1% BSA / 0.3% Triton X-100). The cells were incubated overnight at 4°C. Cells were washed thrice in 1X PBS for 5 mins. for each wash. Cells were incubated in fluorochrome-conjugated secondary antibodies, and diluted in antibody dilution buffer for 1-2 hours at room temperature in the dark. Cells were washed with 1X PBS 3 times for 5 minutes for each wash. The cell was then placed in the slides. The coverslip was mounted with Prolong® Gold Antifade Reagent (#9071, Cell Signal) and Prolong® Gold Antifade Reagent with DAPI. The slides were observed with a fluorescent microscope at the appropriate excitation wavelength.

NMDA induction on dorsal root ganglion neuron: The differentiated DRG neuron was then isolated to receive NMDA to induce DRG neuron activation through NMDAR. Cells were divided into seven groups, with four replications in each group. The media were replaced with new media without the addition of NMDA in the control group, and the other group received 10, 20, 40, 60, 80, and 100 µM NMDA. This study was under Mg²⁺ free conditions to obtain free external Mg²⁺ block in the NMDAR (19). After

incubation for 1 minute, the level of the phosphorylated extracellular signal-regulated kinase was measured to investigate the most optimum DRG neuron activation.

Measurement of pERK using the immunocytochemistry assay: Neuron sensitization mark using phosphorylated ERK (pERK) using the immunocytochemistry method using Phospho-p44/42 MAPK (Erk1/2) (Thr202/Tyr204) antibodies (36-8800, Thermo Fisher Scientific, USA). Neurons are differentiated in 24 well-plates. The treated cells were fixed. The aspirated cell medium was added 2-3 mm above the cell surface 4% formaldehyde in 1x PBS. Cells were fixed for 15 minutes at room temperature. The fixative was aspirated, and then the cells were washed three times using 1 X PBS for 5 minutes for each wash. The next stage was immunostaining. Cells were added with 100% cold methanol until submerged (3-5 mm), then incubated for 10 minutes at -20°C and washed in 1x PBS for 5 minutes. Cells were supplemented with blocking buffer 1x PBS/ 5% normal serum / 0.3% Triton™ X-100). The blocking buffer was aspirated, and then the primary antibody was added with a 1:200 dilution in antibody dilution buffer (1X PBS / 1% BSA / 0.3% Triton X-100). The cells were incubated overnight at 4°C. Cells were washed thrice in 1X PBS for 5 min for each wash. Cells were incubated in fluorochrome-conjugated secondary antibodies, and diluted in antibody dilution buffer for 1-2 hours at room temperature in the dark. Cells were washed with 1X PBS 3 times for 5 minutes for each wash. The coverslip was mounted with Prolong® Gold Antifade Reagent (#9071, Cell Signal) and Prolong® Gold Antifade Reagent with DAPI. The slides were observed with a fluorescent microscope at the appropriate excitation wavelength.

NMDA optimum concentration validation to induce DRG neuron activation: After obtaining the most optimum NMDA concentration to induce DRG neuron activation, we did a validation test by measuring Ca²⁺, Δψ_m, and cytosolic ATP concentration. Those three parameters were associated with neuron activation following NMDAR activation.

Intracellular Ca²⁺ level measurement: NMDAR activation followed by increased Ca²⁺ influx. This measurement uses three groups: Control, Optimum NMDA, and Ketamine (100 µM). Ketamine

was used as an NMDAR blocker. Measurement of Ca^{2+} was done based on Pan *et al.* (17). The cells were cultured on a 24-well polystyrene tissue culture microtiter plate coated with gelatin with a density of 1×10^6 cells/ml. Cells were cultured with 1 ml of media per well and incubated at 5% CO_2 , 37°C. Cells were added with 5×10^{-6} M fura-2/AM (F4897-1MG, Sigma-Aldrich, USA) in HBSS for 1 hour at room temperature and under dark conditions.

After that, the cells were washed, and then the cells were fixed in HBSS (or HBSS without calcium) to measure cytosolic calcium ion concentration. Cells were observed using a confocal laser scanning microscope with excitation at 340 and 380 nm wavelengths. The fluorescent image with the filter (515 \pm 25 nm) was taken with a camera connected to the microscope. The data was obtained in the form of the ratio of the intensity of luminescence at the excitation of 340/380 nm (R). We did 40 times calcium measurements in 9 minutes (four times measurements for basal concentration in one minute and thirty-six times after administration of NMDA 80 μM and ketamine 100 μM in 8 minutes). Since the calcium level was dynamic, we compared the calcium level to the basal condition. In the Ca^{2+} influx measurement, we included a 100 μM ketamine group as an NMDAR antagonist to assess the reversible effect of NMDAR activation.

Mitochondrial membrane potential measurement ($\Delta\psi\text{m}$): The mitochondrial membrane potential staining method is based on Pendergrass *et al.* (17). Treated cells were harvested by trypsinization and washed two times in PBS. Cells were resuspended in DMEM supplemented with 10% FBS, 25 mM HEPES medium, and stained with 40 nM MitoTracker Green (M7514, Thermo Fisher Scientific, USA) for 60 min, at 37°C. The unbound dye was washed with DMEM containing 10% FBS at 37°C. The luminescence of the dye was analyzed using a confocal laser scanning microscope (CLSM) with excitation at 490 nm and emission at a wavelength of 516 nm.

Cytosolic ATP concentration measurement: ATP measurement using ATP Assay Kit (Colorimetric/Fluorometric) (ab83355, Abcam, USA). The ATP measurement was initiated by making a standard curve according to the product instructions. After treatment, cells were incubated for 24 hours with

5% CO_2 at 37°C for intracellular ATP measurement. A total of 1×10^6 cells were harvested and used for analysis. Cells were washed with PBS. Cells were resuspended in 100 μL ATP assay buffer. Cells were homogenized. Cells were centrifuged for 5 minutes at 4°C and a speed of 13,000 g. The supernatant was put into a new tube and stored on ice. The cells were then deproteinated to prevent enzyme contamination. Cold 4 M perchloric acid (PCA) was added to the homogenate until the solution had a final concentration of 1 M, then homogenized. Samples were incubated for 5 minutes on ice. The sample was centrifuged for 2 minutes at 13,000 g (10,000 rpm) at 4°C, and the supernatant was transferred to a new tube. The supernatant volume was measured. Excess PCA was precipitated by adding 2 M cold KOH equivalent to 20-35% of the sample volume (sample + PCA). This neutralization process was carried out by adjusting the pH using 0.1 M KOH or PCA with a pH ranging from 6.5 to 8.0. Samples were centrifuged at 13,000 g for 15 minutes at 4°C, then the supernatant was taken. This sample was then used for measuring deproteinization dilution factor (DDF), using the following formula:

$$\text{DF} = \frac{\text{initial volume} + \text{volume PCA} + \text{volume KOH} (\mu\text{L})}{\text{initial volume in PCA}}$$

A total of 50 μL ATP reaction mix and background control mix for each group were prepared. 50 μL of the reaction mix was added to each well of the 96-well plate containing the standard and sample. 50 μL of background reaction mix was also added to the background control sample. Samples were homogenized and incubated at room temperature for 30 minutes in the dark. Samples were measured using a microplate reader at 570 nm. The amount of intracellular ATP is measured using the equation:

$$\text{ATP concentration} = \left(\frac{B}{V} \times D \right) \times \text{DDF}$$

B: the amount of ATP in the sample calculated based on the standard curve

V: volume of sample added in well

D: sample dilution factor (if dilution is carried out to adjust within the measurement range)

DDF: deproteinization dilution factor

Statistical analysis: Data were analyzed with SPSS

Statistics 20.0 software (SPSS Inc., Chicago, Illinois, USA). The MAP2 and pERK were analyzed using the One-Way ANOVA and Duncan Post Hoc Test. Intracellular calcium level was descriptively presented. The mitochondrial membrane potential and cytosolic ATP were tested using an independent t-test. This study used $\alpha=5\%$ with a significance of $p<0.05$.

Results

Differentiated DRG neuron culture: The differentiated DRG neuron culture shows a significant MAP2 expression on day 5 (197.31 ± 19.90 AU) compared to control and another day ($p<0.05$). The confocal image on day five also shows a higher intensity of green fluorescence than on day 0 (Fig. 1). From morphological observation, differentiated DRG neurons showed elongation of axons from the soma (cell body). On day 0, the culture cell only contains the soma without dendrites or axons. The observation on day five shows (Fig. 2). Based on the morphological and biomolecular examination, we use DRG neuron culture differentiated on day 5 to receive further treatment.

NMDA effect on phosphorylated extracellular signal-regulated kinase (pERK): The phosphorylated extracellular signal-regulated kinase is associated with neuron activity biomarkers. This study showed that the administration of $80 \mu\text{M}$ NMDA on DRG neurons significantly had the highest pERK expression (147.27 ± 0.37 AU) compared to the control

(98.49 ± 12.06 AU) ($p<0.05$) and other treatment groups. The administration of $100 \mu\text{M}$ NMDA significantly had the lowest pERK (2.06 ± 0.07 AU) compared to the other group ($p<0.05$) (Fig. 3). The expression of pERK observed using a fluorescent microscope can be seen in Fig. 3. NMDA $80 \mu\text{M}$ show the highest green fluorescent intensity. The highest pERK intensity shows the optimum neuron activation. Therefore, NMDA $80 \mu\text{M}$ is the most optimum concentration to increase pERK intensity in the DRG neuron.

NMDA effect on Ca^{2+} influx, $\Delta\psi\text{m}$, and cytosolic ATP concentration: To validate whether NMDA $80 \mu\text{M}$ could induce DRG neuron activation following NMDAR activation, we examine Ca^{2+} influx. Ca^{2+} influx is the downstream cascade following NMDAR activation. In the Mg^{2+} free medium, administration of $80 \mu\text{M}$ NMDA shows a significant elevation in calcium influx in the initial NMDA administration compared to the basal level. The control group shows no significant fluctuation. The control group showed a more stable calcium level and no significant fluctuation than the basal level. Ketamine administration as an NMDAR blocker also shows no significant calcium fluctuation compared to the basal level (Fig.4).

We also examine the $\Delta\psi\text{m}$ and cytosolic ATP concentration related to neuron activation. The induction of NMDA $80 \mu\text{M}$ exhibits an increase of $\Delta\psi\text{m}$ from 76.19 ± 5.09 AU in the control group to 109.24 ± 6.43 AU in the NMDA group ($p<0.05$) (Fig.

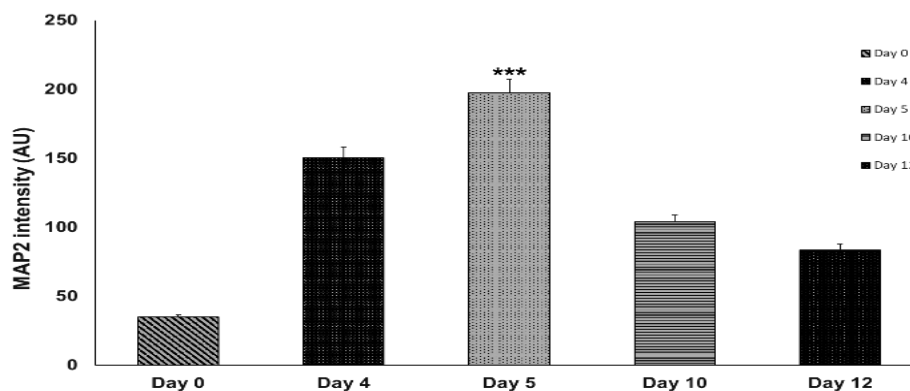


Figure 1. MAP2 expression on the neuron culture. Observation on day 5 shows a high expression of MAP2. The ^{abc} notation indicates statistical differences between groups.

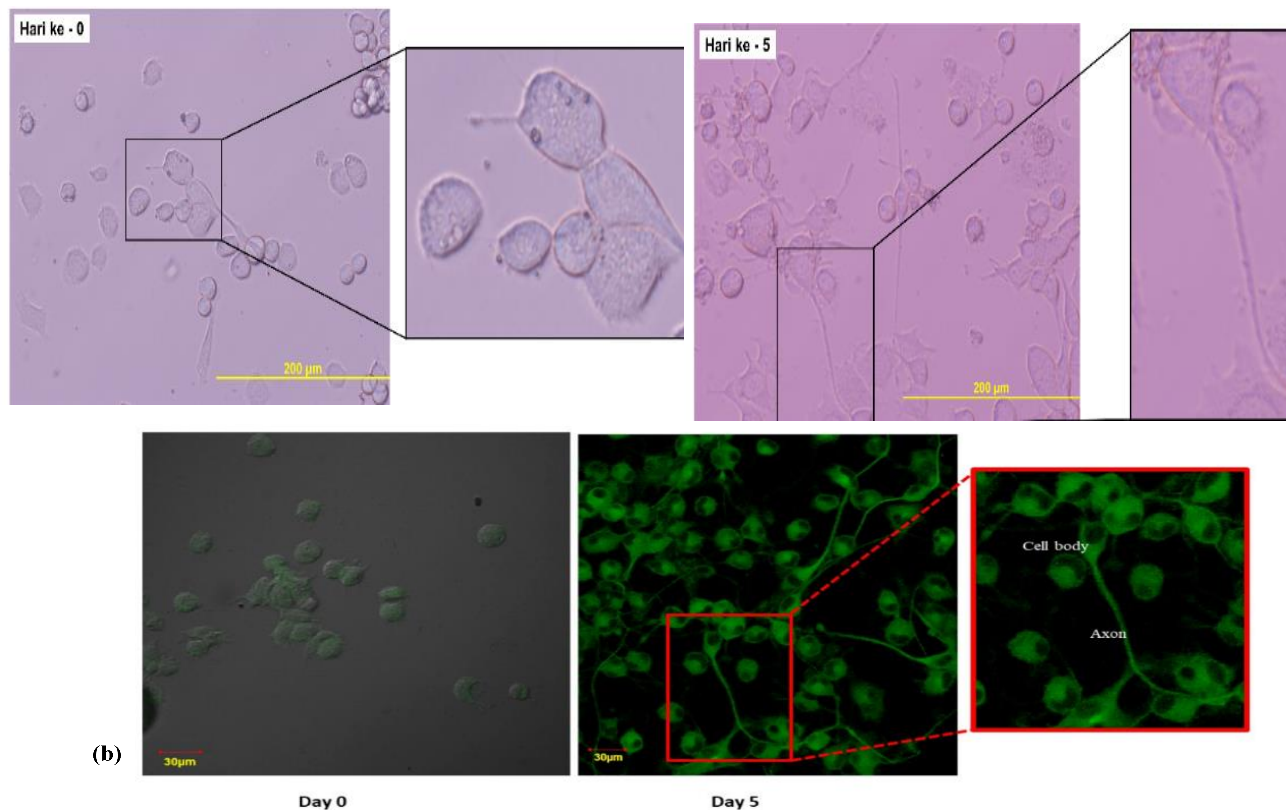


Figure 2. Neurons on day 5 show morphological characteristics of neurons including the elongation of axons. A). Microscopic observation shows the development of the neuron from day 0 to day 5 B). Fluorescent imaging on day 5 shows well-differentiated DRG neurons. *significantly different ($p < 0.05$).

5A). Cytosolic ATP concentration measurement found that there is a significant depletion in the cytosolic ATP

concentration from 0.0228 ± 0.0004 mM (control) to 0.0199 ± 0.0004 nM (NMDA $80 \mu\text{M}$ group) ($p < 0.05$)

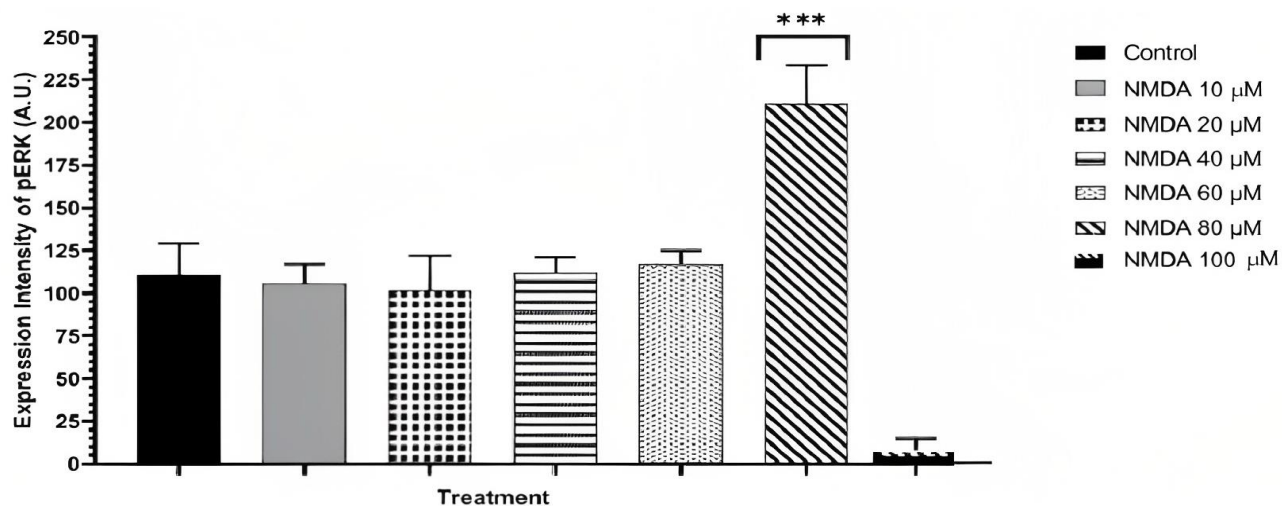


Figure 3. Expression of pERK as a biomarker of neuronal sensitization. NMDA $80 \mu\text{M}$ significantly had the highest pERK expression compared to control and other treatments. *significantly different ($p < 0.05$).

(Fig.5C).

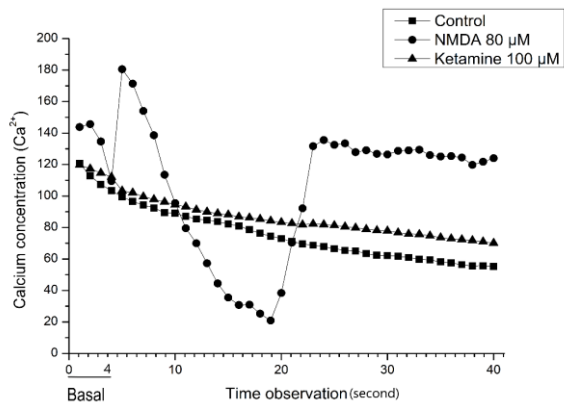


Figure 4. The administration of NMDA 80 μM significantly increases calcium level at the initial time of 80 μM NMDA introduction compared to basal level.

Discussion

In the cellular study of chronic pain, NMDAR activation is essential to induce neuron activation (20). Glutamate receptor activation increases neuron activity by inducing membrane depolarization, activating the chronic pain pathway (21, 4). Neuron activation is indicated by pERK expression (5). No study compares the different concentrations of NMDA to induce neuron activation through the NMDAR pathway. This study uses differentiated DRG neurons marked by MAP2 neuronal biomarkers. MAP2 is highly expressed in the DRG neuron's cell body and axon (22).

Administration of 80 μM NMDA on DRG neurons significantly had the highest pERK expression compared to the control and treatment groups of NMDA 10, 20, 40, 60, and 100 μM . This indicates that the optimum DRG neuron activation was obtained by 80 μM NMDA induction. pERK is one of the MAPKs used as a biomarker of nociceptive neuron activation (23). pERK is expressed after extracellular signal-regulated kinase phosphorylation by MAP or ERK kinase after exposure to a noxious stimulus (6). ERK plays a role in the neuron's plasticity, central sensitization, and synapses underlie pain hypersensitivity (4). The accumulation of pERK in neurons of the dorsal horn is important in central sensitization (chronic pain) and increases the sensitivity of the neurons responsible for persistent

pain. In addition, pERK can also exhibit primary sensory neuron activity in the DRG (24). The administration of 100 μM NMDA significantly shows the lowest level of pERK expression compared to control and other concentrations. The low level of pERK far from control might be caused by neurotoxicity-related neuron death.

The use of NMDA in the neuronal culture must consider the optimum concentration to avoid neurotoxicity. Simoes *et al.* show a decrease in neuron culture viability after administration of NMDA 100 μM (25). This study also supports the previous study in which NMDA concentration starting from 100 μM should be avoided in the neuronal culture due to the possibility of neurotoxicity (26). Therefore, we demonstrate that NMDA 80 μM is the optimum concentration to induce neuron sensitization in DRG neuron culture with the highest pERK expression. The high expression of pERK induces post-translational regulation, such as AMPAR and NMDAR enhancement in the neuronal membrane, promoting long-term potentiation. ERK also regulates the transcription factor cAMP-response element binding protein (CREB) to promote transcription of NK-1, prodynorphin, and other genes (Cox-2, c-fos, pro-Dyn, TrkB, Zif268), which induce and maintain central sensitization (6).

To validate whether 80 μM NMDA could induce neuron activation, we assess the downstream reaction following NMDAR activation. We assess Ca^{2+} influx, potential membrane mitochondria, and cytosolic ATP concentrations. In the Mg^{2+} free medium, we found a significant influx of Ca^{2+} in the DRG neuron after 80 μM NMDA induction. The administration of ketamine as an NMDAR blocker shows no significant fluctuation in the Ca^{2+} . The activation of NMDAR increases Ca^{2+} influx, which functions as a secondary messenger in the ERK pathway (25). Calcium mediates ERK activation by activating the upstream cascade, including protein kinase-c (PKC), Raf-1, and MEK (4). This is per our result, where the administration of NMDA significantly increases Ca^{2+} compared to the basal level. Calcium also activates calmodulin-dependent kinase II (CaMKII) which increases AMPAR conductivity and AMPAR transport from the intracellular store to the membrane (27). The increased

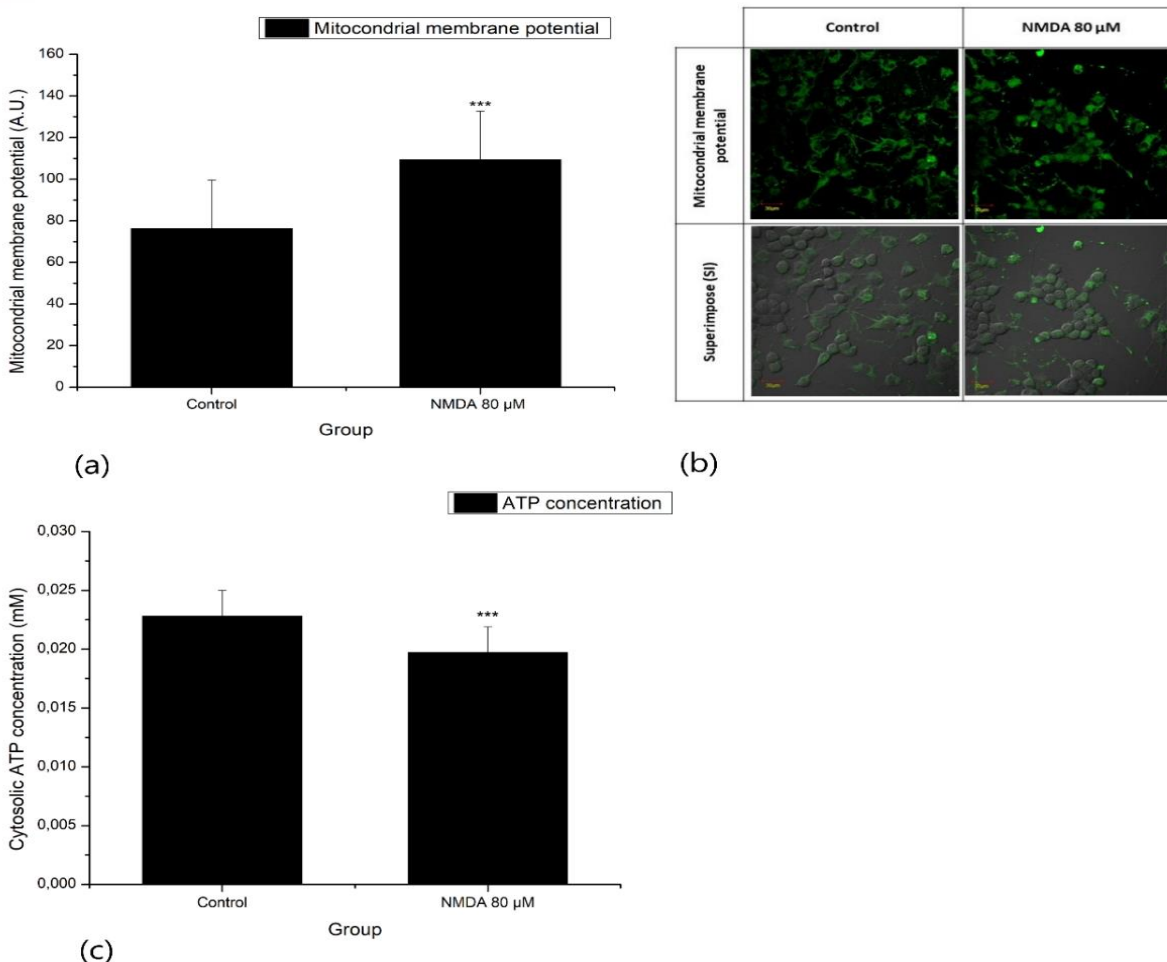


Figure 5. A). The administration of 80 μ M NMDA increases mitochondrial membrane potential B). 80 μ M NMDA shows deeper green fluorescent C). The administration of 80 μ M NMDA decreases intracellular ATP concentration in the neuron DRG. *significantly different ($p < 0.05$). Description: Superimpose (SI): description of the combined observations of mitochondrial membrane potential and DIC (differential interference contrast) observations. Magnification: 400X.

number of NMDAR and AMPAR in the neuron membrane increases and maintains central sensitization (4).

We also measure the mitochondrial membrane potential and cytosolic ATP concentration since neuron activation affects neuronal energy generation. Mitochondria have five main functions: energy generation, reactive oxygen species, mitochondrial permeability transition, cell death, and calcium metabolism (28). Increase intracellular Ca^{2+} after mitochondria absorb NMDAR activation through mitochondrial calcium uniporter (MCU) to regulate energy/ATP generation. Previous studies demonstrate increased mitochondrial calcium influx following NMDAR activation (29). In this study, NMDA 80 μ M administration also shows elevation in $\Delta\psi_m$.

Mitochondrial membrane potential is associated with mitochondrial activity in ATP production (29). A decrease or damage to the mitochondrial membrane can cause a decrease in ATP production (30). This study result shows an increase $\Delta\psi_m$ indicating increased neuron activity associated with increased energy demand. Neurons respond to the high energy demand by increasing mitochondrial activity in energy generation (7).

This study also reveals the cytosolic ATP depletion after NMDA 80 μ M administration. Activated neurons experience high ATP consumption (31). In activated neurons, ATP is used for neurotransmission activity (29). This high ATP consumption is explained by the previous *in-vitro* study, which reveals cytosolic ATP depletion in

neurons after exposure to glutamate and high-frequency electricity. This depletion indicates a high ATP usage in the activated neuron (33).

This result underlies that NMDA 80 μM could induce DRG neuron activation, which is demonstrated by the increase in pERK expression, as well as activate the downstream process following NMDAR activation, including increased calcium influx, increased mitochondrial membrane potential, and cytosolic ATP concentration depletion. This result could be beneficial in establishing a cellular study involving NMDA as a DRG neuron activation inducer through the NMDAR pathway. This result is also beneficial in the in-vitro study, which targets neuron activation-NMDAR dependent as potential chronic pain target therapy.

However, this study has limitations. Since this study aims to find the most optimum NMDA concentration to induce DRG neuron activation through the NMDAR pathway, we did not compare the result with other agonists such as glutamate, glycine, D-cycloserine, and other agonists. Therefore, further study can be done to compare the NMDAR agonist role in pERK expression, especially in the in-vitro study involving DRG neurons.

Conclusion

In summary, NMDA 80 μM is the optimum concentration to induce DRG neuron activation through the NMDA receptor pathway. NMDA 80 μM also affects another downstream process following NMDAR activation, including an increase in intracellular Ca^{2+} influx, an increase $\Delta\psi\text{m}$, and a decrease in cytosolic ATP concentration related to neuron activation.

Acknowledgment

None.

Conflicts of Interest

The authors declare that they have no conflict of interest.

References

1. Traynelis SF, Wollmuth LP, McBain CJ, Menniti FS, Vance KM, Ogden KK, et al. Glutamate receptor ion channels: structure, regulation, and function. *Pharmacol Rev.* 2010;62(3):405-96.
2. Paoletti P, Neyton J. NMDA receptor subunits: function and pharmacology. *Curr Opin Pharmacol.* 2007;7(1):39-47.
3. Iacobucci GJ, Popescu GK. NMDA receptors: linking physiological output to biophysical operation. *Nat Rev Neurosci.* 2017;18(4):236-49.
4. Ji RR, Gereau RWt, Malcangio M, Strichartz GR. MAP kinase and pain. *Brain Res Rev.* 2009;60(1):135-48.
5. Dai Y, Iwata K, Fukuoka T, Kondo E, Tokunaga A, Yamanaka H, et al. Phosphorylation of extracellular signal-regulated kinase in primary afferent neurons by noxious stimuli and its involvement in peripheral sensitization. *J Neurosci.* 2002;22(17):7737-45.
6. Gao YJ, Ji RR. c-Fos and pERK, which is a better marker for neuronal activation and central sensitization after noxious stimulation and tissue injury? *Open Pain J.* 2009;2:11-7.
7. Safiulina D, Kaasik A. Energetic and dynamic: how mitochondria meet neuronal energy demands. *PLoS Biol.* 2013;11(12):e1001755.
8. Shetty PK, Galeffi F, Turner DA. Cellular Links between Neuronal Activity and Energy Homeostasis. *Front Pharmacol.* 2012;3:43.
9. Davis GW. Not Fade Away: Mechanisms of Neuronal ATP Homeostasis. *Neuron.* 2020;105(4):591-3.
10. Krames ES. The role of the dorsal root ganglion in the development of neuropathic pain. *Pain Med.* 2014;15(10):1669-85.
11. Haberberger RV, Barry C, Dominguez N, Matusica D. Human Dorsal Root Ganglia. *Front Cell Neurosci.* 2019;13:271.
12. Berta T, Qadri Y, Tan PH, Ji RR. Targeting dorsal root ganglia and primary sensory neurons for the treatment of chronic pain. *Expert Opin Ther Targets.* 2017;21(7):695-703.
13. Ahimsadasan N, Reddy V, Khan Suheb MZ, Kumar A. Neuroanatomy, Dorsal Root Ganglion. *StatPearls. Treasure Island (FL): StatPearls Publishing. Copyright © 2023, StatPearls Publishing LLC.; 2023.*
14. Chang HR, Kuo CC. The activation gate and gating mechanism of the NMDA receptor. *J Neurosci.* 2008;28(7):1546-56.
15. Chen S, Xu D, Fan L, Fang Z, Wang X, Li M. Roles of N-Methyl-D-Aspartate Receptors (NMDARs) in Epilepsy. *Front Mol Neurosci.* 2021;14:797253.
16. Furukawa H, Singh SK, Mancusso R, Gouaux E. Subunit arrangement and function in NMDA receptors. *Nature.* 2005;438(7065):185-92.
17. Pendergrass W, Wolf N, Poot M. Efficacy of MitoTracker Green and CMXrosamine to measure changes in mitochondrial membrane potentials in living cells and tissues. *Cytometry A.* 2004;61(2):162-9.
18. Pastori V, D'Aloia A, Blasa S, Lecchi M. Serum-deprived differentiated neuroblastoma F-11 cells express functional dorsal root ganglion neuron properties. *PeerJ.* 2019;7:e7951.
19. Clarke RJ, Johnson JW. NMDA receptor NR2 subunit dependence of the slow component of magnesium unblock. *J*

- Neurosci. 2006;26(21):5825-34.
20. Ferrari LF, Lotufo CM, Araldi D, Rodrigues MA, Macedo LP, Ferreira SH, et al. Inflammatory sensitization of nociceptors depends on activation of NMDA receptors in DRG satellite cells. *Proc Natl Acad Sci U S A*. 2014;111(51):18363-8.
21. Westergard T, McAvoy K, Russell K, Wen X, Pang Y, Morris B, et al. Repeat-associated non-AUG translation in C9orf72-ALS/FTD is driven by neuronal excitation and stress. *EMBO Mol Med*. 2019;11(2).
22. Gumy LF, Katrukha EA, Grigoriev I, Jaarsma D, Kapitein LC, Akhmanova A, et al. MAP2 Defines a Pre-axonal Filtering Zone to Regulate KIF1- versus KIF5-Dependent Cargo Transport in Sensory Neurons. *Neuron*. 2017;94(2):347-62.e7.
23. Kondo M, Shibuta I. Extracellular signal-regulated kinases (ERK) 1 and 2 as a key molecule in pain research. *J Oral Sci*. 2020;62(2):147-9.
24. Hung CH, Lee CH, Tsai MH, Chen CH, Lin HF, Hsu CY, et al. Activation of acid-sensing ion channel 3 by lysophosphatidylcholine 16:0 mediates psychological stress-induced fibromyalgia-like pain. *Ann Rheum Dis*. 2020;79(12):1644-56.
25. Khasabov SG, Simone DA. Loss of neurons in rostral ventromedial medulla that express neurokinin-1 receptors decreases the development of hyperalgesia. *Neuroscience*. 2013;250:151-65.
26. Simões AP, Silva CG, Marques JM, Pochmann D, Porciúncula LO, Ferreira S, et al. Glutamate-induced and NMDA receptor-mediated neurodegeneration entails P2Y1 receptor activation. *Cell Death Dis*. 2018;9(3):297.
27. Kristensen AS, Jenkins MA, Banke TG, Schousboe A, Makino Y, Johnson RC, et al. Mechanism of Ca²⁺/calmodulin-dependent kinase II regulation of AMPA receptor gating. *Nat Neurosci*. 2011;14(6):727-35.
28. Sui BD, Xu TQ, Liu JW, Wei W, Zheng CX, Guo BL, et al. Understanding the role of mitochondria in the pathogenesis of chronic pain. *Postgrad Med J*. 2013;89(1058):709-14.
29. Alano CC, Beutner G, Dirksen RT, Gross RA, Sheu SS. Mitochondrial permeability transition and calcium dynamics in striatal neurons upon intense NMDA receptor activation. *J Neurochem*. 2002;80(3):531-8.
30. Zorova LD, Popkov VA, Plotnikov EY, Silachev DN, Pevzner IB, Jankauskas SS, et al. Mitochondrial membrane potential. *Anal Biochem*. 2018;552:50-9.
31. Lange SC, Winkler U, Andresen L, Byhrø M, Waagepetersen HS, Hirrlinger J, et al. Dynamic Changes in Cytosolic ATP Levels in Cultured Glutamatergic Neurons During NMDA-Induced Synaptic Activity Supported by Glucose or Lactate. *Neurochem Res*. 2015;40(12):2517-26.
32. Rodrigues RJ, Tomé AR, Cunha RA. ATP as a multi-target danger signal in the brain. *Front Neurosci*. 2015;9:148.
33. Natsubori A, Tsunematsu T, Karashima A, Imamura H, Kabe N, Trevisiol A, et al. Intracellular ATP levels in mouse cortical excitatory neurons varies with sleep-wake states. *Commun Biol*. 2020;3(1):491.